Pflugers Arch - Eur J Physiol (2009) 458:937–952
DOI 10.1007/s00424-009-0672-0

SIGNALING AND CELL PHYSIOLOGY

H_2O_2-mediated modulation of cytosolic signaling and organelle function in rat hippocampus

Florian J. Gerich · Frank Funke · Belinda Hildebrandt · Martin Faßhauer · Michael Müller

Received: 30 October 2008 / Revised: 6 April 2009 / Accepted: 7 April 2009 / Published online: 10 May 2009
© The Author(s) 2009. This article is published with open access at Springerlink.com

Abstract Reactive oxygen species (ROS) released from (dys-)functioning mitochondria contribute to normal and pathophysiological cellular signaling by modulating cytosolic redox state and redox-sensitive proteins. To identify putative redox targets involved in such signaling, we exposed hippocampal neurons to hydrogen peroxide (H_2O_2). Redox-sensitive dyes indicated that externally applied H_2O_2 may oxidize intracellular targets in cell cultures and acute tissue slices. In cultured neurons, H_2O_2 (EC_{50} 118 μM) induced an intracellular Ca^{2+} rise which could still be evoked upon Ca^{2+} withdrawal and mitochondrial uncoupling. It was, however, antagonized by thapsigargin, dantrolene, 2-aminoethoxydiphenyl borate, and high levels of ryanodine, which identifies the endoplasmic reticulum (ER) as the intracellular Ca^{2+} store involved. Intracellular accumulation of endogenously generated H_2O_2—provoked by inhibiting glutathione peroxidase—also released Ca^{2+} from the ER, as did extracellular generation of superoxide. Phospholipase C (PLC)-mediated metabotropic signaling was depressed in the presence of H_2O_2, but cytosolic cyclic adenosine-5′-monophosphate (cAMP) levels were not affected. H_2O_2 (0.2–5 mM) moderately depolarized mitochondria, halted their intracellular trafficking in a Ca^{2+}- and cAMP-independent manner, and directly oxidized cellular nicotinamide adenine dinucleotide (NADH) and flavin adenine dinucleotide ($FADH_2$). In part, the mitochondrial depolarization reflects uptake of Ca^{2+} previously released from the ER. We conclude that H_2O_2 releases Ca^{2+} from the ER via both ryanodine and inositol trisphosphate receptors. Mitochondrial function is not markedly impaired even by millimolar concentrations of H_2O_2. Such modulation of Ca^{2+} signaling and organelle interaction by ROS affects the efficacy of PLC-mediated metabotropic signaling and may contribute to the adjustment of neuronal function to redox conditions and metabolic supply.

Keywords Redox signaling · Autofluorescence · Mitochondrial dysfunction · Intracellular calcium stores · Oxidative stress · Metabotropic signaling

Florian J. Gerich and Frank Funke contributed evenly to this study.

Electronic supplementary material The online version of this article (doi:10.1007/s00424-009-0672-0) contains supplementary material, which is available to authorized users.

F. J. Gerich · F. Funke · B. Hildebrandt · M. Faßhauer · M. Müller (✉)
DFG Research Center Molecular Physiology of the Brain (CMPB), Zentrum für Physiologie und Pathophysiologie, Abteilung Neuro- und Sinnesphysiologie, Georg-August-Universität Göttingen, Humboldtallee 23, 37073 Göttingen, Germany
e-mail: mmuelle7@gwdg.de

Introduction

Mitochondria constantly generate small amounts of superoxide which is rapidly converted to hydrogen peroxide (H_2O_2), that then escapes from the mitochondria into the cytosol and modulates cytosolic redox state [8, 9, 16, 19]. In the presence of transition metals (e.g., Fe^{2+}), H_2O_2 may react in a Fenton reaction forming the reactive hydroxyl radical [14, 35]. At moderate levels, reactive oxygen species (ROS) take part in physiological signaling, by contributing to the adjustment of brain function to cellular metabolism and metabolic supply (for review see [16]). Due to the presence of exposed sulfhydryl (SH)-groups, several ion channels and receptors are modulated by changes in cytosolic redox balance. Examples are NMDA

receptors [2], GABA receptors [48], various K^+ channels [39, 53], voltage-sensitive Ca^{2+} channels [40], and the persistent Na^+ current [25], each of which is well capable of modulating the responsiveness of complex neuronal networks. As a consequence, a variety of neuronal functions is modulated by H_2O_2, including neuronal excitability [42], basal synaptic transmission [5], and long-term potentiation [30, 43].

In earlier studies, typically 1–3 mM H_2O_2 was used to probe, e.g., for the modulation of synaptic function [42]. At that concentration, H_2O_2 also seems to contribute to anoxic/ischemic preconditioning. Recently, we reported that sulfhydryl oxidation, mediated by the oxidant 5,5′-dithio-bis-2-nitrobenzoic acid (DTNB), decreases the susceptibility of rat hippocampal slices to severe hypoxia, as indicated by the delayed occurrence of hypoxia-induced spreading depression (HSD) [26, 27], a phenomenon which resembles an experimental model for ischemic cerebral stroke. This oxidant-mediated postponement of HSD is based on the activation of BK-type K_{Ca} channels; as a result, hippocampal CA1 neurons tolerated severe hypoxia for a longer period of time [26]. A similar postponement of HSD was achieved by application of H_2O_2 (1–5 mM). Even though the propagation velocity of HSD, the extent of tissue invasion, and the massive rise in the extracellular K^+ concentration were not attenuated by H_2O_2 or DTNB, and synaptic recovery upon reoxygenation was not improved [27], the postponement of HSD by H_2O_2 is interesting because H_2O_2—in contrast to DTNB—may be produced endogenously in neuronal networks.

Excessive production or continued presence of ROS and reactive nitrogen species is, however, deleterious because it contributes to the neuronal damage and degeneration associated with pathophysiological conditions such as Parkinson's disease, amyotrophic lateral sclerosis, Down's syndrome, epilepsy, and ischemia/reperfusion injury [1, 10, 24, 32, 52]. In primary cultures of cortical and hippocampal neurons, H_2O_2 depletes cellular adenosine triphosphate (ATP) content [57], and applied for up to 24 h, it mediates apoptotic cell death in a mouse beta-cell line (MIN6N8a) [11].

In search for intracellular oxidation-sensitive targets responding to acute rather than chronic oxidative conditions within the hippocampal network, we therefore asked to what extent intracellular Ca^{2+} concentration ($[Ca^{2+}]_i$), mitochondrial function, and organelle interaction are modulated by H_2O_2. Our methodological focus was on live cell imaging, i.e., the optical detection of changes in $[Ca^{2+}]_i$, redox state, and mitochondrial function. To modulate cytosolic redox state, H_2O_2 was applied extracellularly to hippocampal cell cultures and acute hippocampal tissue slices. While this of course does not mimic highly localized and compartment specific H_2O_2 release, it has, however, been found to be a valid approach to screen for oxidation-sensitive targets in various tissues [9, 11, 42, 57].

We found that H_2O_2 releases Ca^{2+} from the endoplasmic reticulum (ER) via ryanodine as well as inositol trisphosphate (IP3) receptors. Mitochondrial membrane potential ($\Delta\Psi_m$) was only moderately affected, but phospholipase C (PLC)-mediated metabotropic signaling was depressed in the presence of H_2O_2. Furthermore, multiphoton imaging revealed that H_2O_2 halted the intracellular trafficking of mitochondria.

Materials and methods

Preparation

Hippocampal tissue slices were prepared from ether anesthetized male Sprague–Dawley rats of 150-300 g body weight (4–6 weeks of age). Only on a few occasions, acute slices from juvenile rats (p13–15) were used. Following decapitation, the brain was rapidly removed and placed in ice-cold artificial cerebrospinal fluid (ACSF) for 1–2 min. The hemispheres were separated and 400 µm thick slices were cut using a vibroslicer (Campden Instruments, 752M Vibroslice). The hippocampal formation was then isolated from each slice, transferred to a storage chamber (30-33°C, constantly aerated with carbogen [95% O_2–5% CO_2]), and left undisturbed for at least 90 min.

Hippocampal cell cultures were prepared from neonatal rats (2–4 days old) following standard culturing procedures [36]. After decapitation, the brain was removed and placed in ice-cold Hanks' balanced salt solution containing 20% fetal calf serum (FCS, Biochrom). The isolated hippocampi were cut into small pieces and trypsinated (5 mg/ml, 10 min, 37°C); cells were then dissociated and centrifuged (1,500 rpm, 10 min, 4°C). The re-suspended pellet was plated on Matrigel (BD Biosciences)-coated cover slips, which were transferred to four-well culture plates (Nunc); each well contained 600 µl of medium. Cultures were incubated at 37°C in a humidified, 5% CO_2-containing atmosphere. After 24 h, half of the medium was replaced with growth medium (for composition, see "Solutions"); the antimitotic agent cytosine arabinoside (4 µM; Sigma-Aldrich) was added to inhibit growth of glial cells. Medium and growth factors were refreshed after 2–3 days; experiments were performed between 3 and 7 days in culture.

Solutions

Chemicals, unless otherwise mentioned, were obtained from Sigma-Aldrich. The ACSF was composed of (in mM): 130 NaCl, 3.5 KCl, 1.25 NaH_2PO_4, 24 $NaHCO_3$, 1.2 $CaCl_2$, 1.2 $MgSO_4$, and 10 dextrose; aerated with carbogen to adjust pH to 7.4. Minimum essential cell culture medium (Invitrogen) was supplemented with 5 mg/ml glucose, 0.2 mg/ml $NaHCO_3$, and 0.1 mg/ml transferrin (Calbiochem).

For initial plating ("plating medium"), it also contained 10% FCS, 2 mM L-glutamine, and 25 µg/ml insulin. The medium used after day 1 in culture ("growth medium") contained 5% FCS, 0.5 mM L-glutamine, 20 µl/ml B27 50× supplement (Invitrogen), and 100 µg/ml penicillin–streptomycin (Biochrom).

Rhodamine 123 was dissolved in absolute EtOH (20 mg/ml). Fluo-3 (Mobitec) was dissolved as 2 mM stock in a mixture of 90% dimethylsulfoxide (DMSO) and 10% pluronic acid; the latter was added to improve dye loading of the cells. The redox-sensitive dyes hydroethidium (HEt) and 5,6-chloromethyl-2′,7′dichlorodihydrofluorescein diacetate (CM-H_2DCFDA, Invitrogen) were dissolved in DMSO as 10 and 1 mM stocks, respectively, and stored under argon to prevent their oxidation by ambient oxygen. Carbonyl cyanide 4-(trifluoromethoxy) phenylhydrazone (FCCP, Tocris), forskolin, thapsigargin (Tocris), 2-aminoethoxydiphenyl borate (2-APB), and dantrolene were prepared as 5–10 mM stocks in DMSO. 3-Isobutyl-1-methylxanthine (IBMX) was prepared as 500 mM stock in DMSO. Ryanodine (Tocris) was dissolved as 10 mM stock in absolute EtOH. Final DMSO and EtOH concentrations were ≤0.25%. Uridine-5′-trisphosphate (UTP) was prepared as aqueous 10 mM stock. Xanthine (X) was prepared as 500 mM stock in 1 M NaOH, and xanthine oxidase (XO) was purchased as a 44 mg/ml ammonium sulfate suspension. 1,4-dithio-DL-threitol (DTT, Fluka), mercaptosuccinic acid (MCS), $FeSO_4$, deferoxamine, diethyldithiocarbamic acid (DEDTC), and H_2O_2 (30% aqueous stock solution) were directly added to the respective solutions. Cyanide (CN^-, sodium salt) and glutamate (sodium salt) were dissolved as aqueous 1 M stocks and kept frozen at −20°C. CN^- dilutions were prepared freshly immediately before use.

Optical recordings

Optical recordings of cytosolic Ca^{2+}, ROS and cyclic adenosine-5′-monophosphate (cAMP) levels, mitochondrial membrane potential ($\Delta\Psi_m$), and nicotinamide adenine dinucleotide (NADH)/flavin adenine dinucleotide (FAD) autofluorescence were performed with a computer-controlled fluorescence imaging system composed of a monochromatic light source (Polychrome II, Till Photonics, Gräfelfing, Germany) and a highly sensitive CCD camera (Imago QE, PCO Imaging, Kelheim, Germany). Previously, we have shown that such CCD camera-based imaging is capable of visualizing structures down to a depth of ~140 µm from the tissue slice surface [21]. Imaging of tissue slices and cell cultures was performed in a submersion-style chamber (33–35°C) using ×40 0.8 NA (Zeiss Achroplan) and ×63 1.0 NA (Zeiss Apochromat) water immersion objectives, respectively. HEt, Rh123, as well as fluo-3, and CM-H_2DCFDA were excited at 470, 480, and 485 nm, respectively, and fluorescence emission was recorded using a 505-nm beam-splitter and a 535/35-nm bandpass filter. Cellular NADH and FAD levels were monitored simultaneously by alternate excitation at 360 nm (NADH) and 445 nm (FAD), and autofluorescence was recorded using a 450-nm beam-splitter and a 510/80-nm bandpass filter [17, 19, 22]. For all optical experiments, the changes in fluorescence emission (peak minus actual baseline) were normalized to the actual pretreatment baseline. In addition, in the case of drug treatments, the fluorescence changes observed in the presence of the drug were also normalized to the control responses recorded earlier in the respective preparation to quantify the drug effects.

Changes in cytosolic cAMP levels were monitored using a genetically encoded cyan fluorescent protein (CFP)/yellow fluorescent protein (YFP) fluorescence resonance energy transfer (FRET) construct containing the cAMP-binding element exchange protein directly activated by cAMP (Epac) [44]. Dr. Kees Jalink (The Netherlands Cancer Institute) kindly provided us with an improved version (CFP-Epac (delta-DEP, CD)-Venus) of the construct in which YFP had been replaced by the Venus variant of YFP, resulting in improved FRET efficiency, higher UV stability and less pH sensitivity [59]. For expression of the construct, hippocampal cell cultures were transfected by electroporation (Nucleofector, Amaxa, Gaithersburg, MD, USA). Cells were dissociated, centrifuged (1,000/min, 5 min), and resuspended in 100 µl nucleofector medium (Amaxa) containing 3 µg DNA, and the efficiency-maximized transfection program (G-13) was used for electroporation. Sufficient expression levels were obtained within 48 h after transfection. Technically, this FRET construct reports increased cAMP levels and the resulting binding of cAMP by a decrease in FRET efficiency [44]. Excitation was performed at 430 nm (DC458 nm beam-splitter) to directly excite CFP. Donor (CFP) and acceptor (YFP) emissions were monitored simultaneously using an optical image splitter device (Dual-View™, Optical Insights, Tucson, AZ, USA, beam-splitter 505 nm, CFP emitter 483/32 nm, YFP emitter 535/30 nm) that spectrally separates CFP and YFP fluorescence and projects the resulting half images one onto either side of the CCD camera chip.

Single mitochondria were visualized with a custom-built two-photon laser scanning system as described earlier [37, 38]. Briefly, the system is composed of an upright microscope (Axioscope 2-FS, Zeiss), a Ti/sapphire laser with broad-band optics (Millenia Vs-pumped Tsunami, Spectra Physics), an infrared-optimized water immersion objective (IR-Achroplan ×63/0.9 W, Zeiss), and a custom-built scan-head with galvanometric scanners (G120 series, General Scanning Inc.). Fluorescence emission is collected by wide-field detection using a photomultiplier tube (R1527, Hamamatsu) [38].

Cellular ATP content was determined from acute slices as reported earlier [22]. Control and H_2O_2 treated slices

(5 mM, 20–25 min) were transferred to perchloric acid (8%) and homogenized by 5-10 s of sonication (Cell Disruptor W-220F, Heat Systems-Ultrasonics). ATP levels were determined in a coupled reaction of glucose-6P-dehydrogenase and hexokinase, by monitoring spectrophotometrically the formation of reduced $NADPH_2$ [22, 33].

Statistics

To ensure independence of observations, each experimental treatment was performed on at least three different rats. Numerical values are represented as mean ± standard deviation. Significance of the observed changes was tested using a two-tailed, unpaired Student's *t* test. In the case of paired observations, a one-sample *t* test was used to compare normalized drug effects against pretreatment control conditions, defined as unity or as 100%. In the diagrams, significant changes are marked by asterisks (*$p<0.05$; **$p<0.01$).

Results

With our interest being focused on the immediate effects of H_2O_2, i.e., the cellular responses occurring on the time scale of minutes, rather than several hours, we characterized the acute effects of externally applied H_2O_2 in hippocampal neurons on the single cell level (cell cultures) as well as on the tissue level (acute tissue slices). We determined the time course of H_2O_2-mediated oxidation of intracellular targets and probed for changes in $[Ca^{2+}]_i$, a possible modulation of metabotropic signaling cascades, as well as changes in the polarization, metabolism, and subcellular distribution of mitochondria.

Time course of H_2O_2-mediated oxidation

In initial experiments, we used redox-sensitive dyes to determine the time course of H_2O_2-mediated oxidation of intracellular targets. In cultured hippocampal neurons and acute hippocampal tissue slices, external application of H_2O_2 oxidized within 1–2 min the redox-sensitive dyes HEt and CM-H_2DCFDA, as indicated by an increase in fluorescence emission. In cultured neurons, H_2O_2 (0.5 mM, 2–3 min) increased HEt fluorescence by 5.9± 2.7% (n=8, Fig. 1a). In acute hippocampal slices (adult rats), the concentration as well as the duration of H_2O_2 application (1 mM, 5–8 min) was increased to compensate for the slower diffusion of H_2O_2 into the slice. On average,

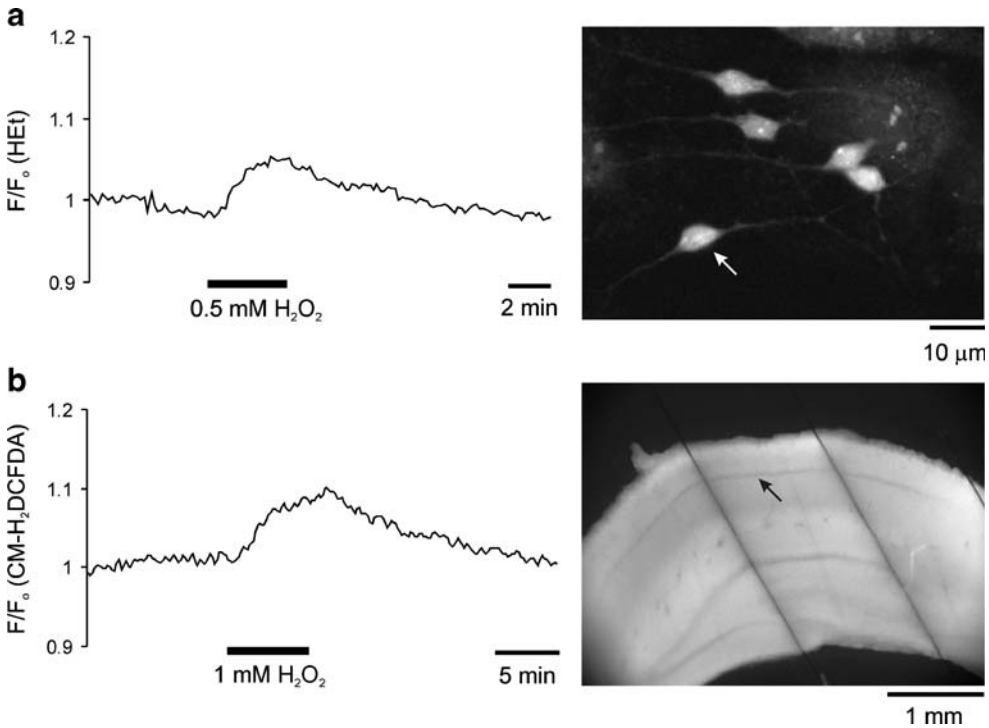

Fig. 1 Oxidation of redox-sensitive dyes confirms that externally applied H_2O_2 readily oxidizes intracellular targets. **a** Application of H_2O_2 induced within less than 1 min a clear increase in hydroethidium (*HEt*; 10 µM, 30 min bulk loaded) fluorescence in cultured hippocampal neurons, which indicates oxidation of the cytosolic dye. The plotted HEt fluorescence changes were determined within the soma of the indicated neuron and are normalized to pretreatment baseline conditions (F/F_0). **b** Acute hippocampal tissue slices bulk loaded with 5,6-chloromethyl-2′,7′dichlorodihydrofluorescein diacetate (*CM-H₂DCFDA*; 5 µM, 30 min) responded within 1 min to H_2O_2 with a clear fluorescence increase. The plotted fluorescence was averaged within a small rectangular region of interest (~40×40 µm) in the CA1 region (*stratum pyramidale*; *arrow mark*) of the displayed tissue slice. The slice was immobilized in a submersion chamber by a mesh of fine nylon strings

such treatment increased CM-H_2DCFDA fluorescence by 8.9±1.9% (n=4; Fig. 1b). Since both dyes are oxidized irreversibly, the decrease in HEt and CM-H_2DCFDA fluorescence upon H_2O_2 withdrawal does not reflect normalization of cellular H_2O_2 levels, but rather bleaching or cellular extrusion of the oxidized dye.

H_2O_2-mediated changes in cytosolic Ca^{2+} levels

In cultured hippocampal neurons (dissociated cultures) loaded with the Ca^{2+} indicator fluo-3 (5 µM, 30–40 min), application of H_2O_2 (2-3 min) consistently induced a moderate increase in $[Ca^{2+}]_i$ that started with a delay of about 1 min and developed rather slowly. This time course is similar to the responses of the redox-sensitive dye HEt that was oxidized in cultured cells within 1 min upon H_2O_2 administration (Fig. 1a). The H_2O_2-mediated Ca^{2+} rise could be evoked repeatedly and was dose-dependent (Fig. 2a). Applied in concentrations from 20 µM to 5 mM, H_2O_2 increased fluo-3 baseline fluorescence by 6.8±4.1% (n=19) and 42.1±20.2% (n=46), respectively, and the corresponding Hill plot yields an EC_{50} of 118 µM H_2O_2 (Fig. 2a, b). In comparison, application of 50 µM glutamate—our standard test to verify cell viability—induced a large, rapid intracellular Ca^{2+} rise, averaging 218±115% (n=220, data not shown). The H_2O_2-induced Ca^{2+} rise could still be evoked upon withdrawal of extracellular Ca^{2+} (Fig. 2c, d), now averaging 14.8±7.8% (200 µM H_2O_2), 35.3±13.3% (1 mM H_2O_2), and 30.9±15.9% (5 mM H_2O_2, n=41 each), which indicates release of Ca^{2+} from intracellular stores. Only at the highest concentration of H_2O_2 tested (5 mM), the responses in Ca^{2+}-free solution were slightly less intense than in control solutions (Fig. 2d).

In the next set of experiments, we pharmacologically targeted mitochondria and the ER to identify the Ca^{2+} stores modulated by H_2O_2. To prevent Ca^{2+} influx from the extracellular space, these experiments were consistently performed in Ca^{2+}-free solutions. H_2O_2 was applied up to three times. The first H_2O_2 response was recorded under

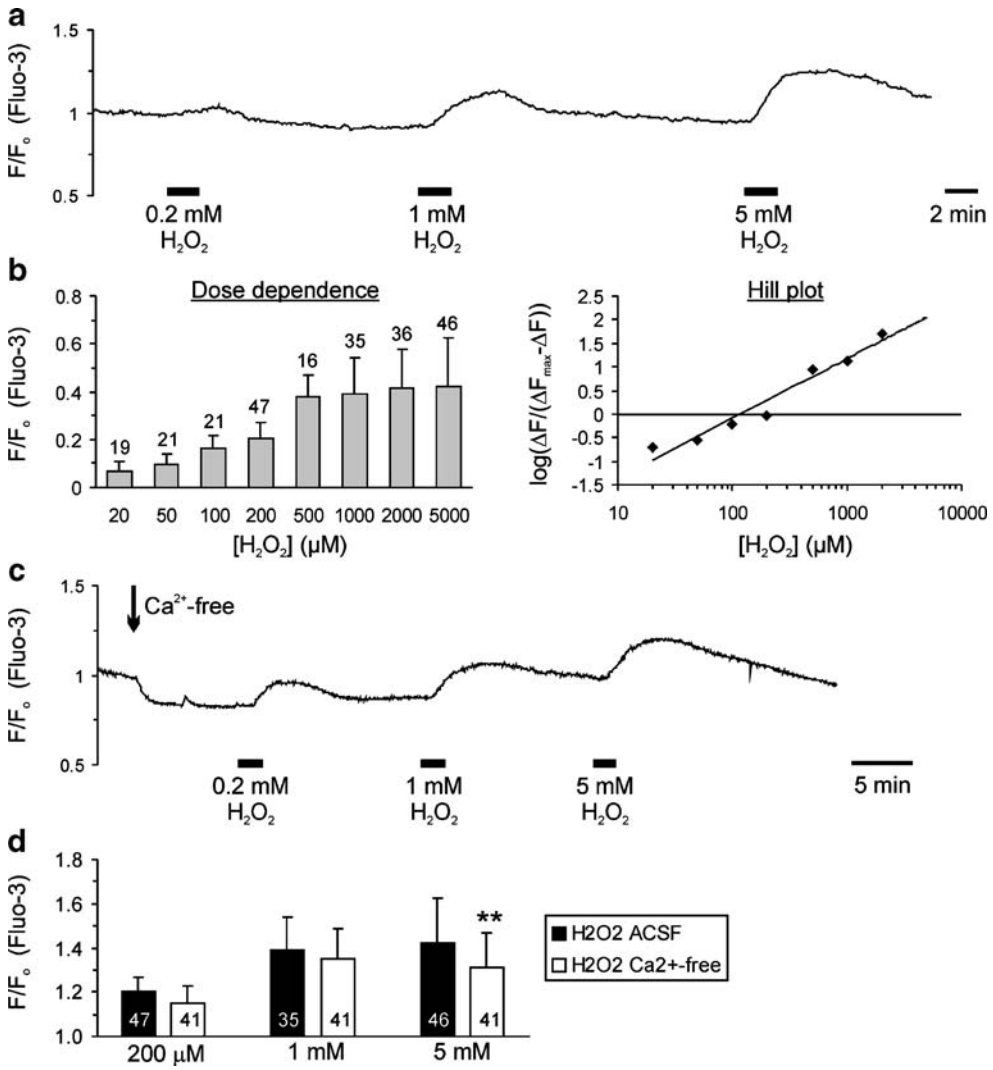

Fig. 2 H_2O_2 induces a moderate increase in $[Ca^{2+}]_i$ that persists in Ca^{2+}-free solutions. **a** In cultured hippocampal neurons, H_2O_2 induced a moderate, reversible, and dose-dependent increase in fluo-3 fluorescence, indicating a rise in $[Ca^{2+}]_i$. The plotted fluo-3 emission was quantified in the soma and normalized to pretreatment baseline fluorescence (F/F_0). **b** Dose dependence of the H_2O_2-induced Ca^{2+} changes. In the corresponding Hill plot, the intercept of the log $[H_2O_2]$ axis corresponds to an EC_{50} of 118 µM H_2O_2. **c** The H_2O_2-induced increase in $[Ca^{2+}]_i$ could still be elicited upon withdrawal of extracellular Ca^{2+}, suggesting Ca^{2+} release from intracellular stores. The *arrow mark* indicates the time point at which extracellular Ca^{2+} was withdrawn for the remaining duration of the experiment. **d** Comparison of the H_2O_2-induced Ca^{2+} transients observed in control (*ACSF*) and Ca^{2+}-free solutions. Data are plotted as mean ± standard deviation, and the number of cells is indicated in the *respective bars*. *Asterisks* mark significantly different changes as compared to ACSF (**P<0.01)

control conditions, the second upon drug treatment, and in most experiments H_2O_2 was applied a third time after the drugs had been washed out again. Under control conditions, the single Ca^{2+} transients evoked by repetitive administration of H_2O_2 (200 µM, 2–3 min) did not differ from each other (Fig. 3a, c). Drug-induced changes were normalized to the previously recorded control response and the significance was tested by unpaired Student's *t* tests, comparing the drug effects with the repetitive administration of H_2O_2 in control solutions (for summary see Table 1 and Fig. 4e). Uncoupling of mitochondria by the protonophore FCCP (1 µM) caused a moderate increase in $[Ca^{2+}]_i$ which reflects the release of the sequestered Ca^{2+} from the depolarizing mitochondria [51]. Yet FCCP treatment did not significantly affect the H_2O_2-induced Ca^{2+} transients, which still averaged 81.4±34.1% of the previously recorded control response (n=32, Figs. 3b and 4e).

To elucidate an involvement of the ER in the H_2O_2-induced Ca^{2+} release, the cells were pretreated with thapsigargin (1 µM, 5–10 min), an inhibitor of the sarco/endoplasmic reticulum Ca^{2+}-ATPase (SERCA). Since Ca^{2+} depletion of the ER may be rather slow in response to thapsigargin only, we applied H_2O_2 twice in the presence of thapsigargin to accelerate Ca^{2+} depletion. The first Ca^{2+} transient evoked by H_2O_2 under these conditions, i.e., the one meant to empty the ER [58], was not significantly decreased. Yet, in the majority of cells (70%), the Ca^{2+} rise elicited by the second H_2O_2 application was noticeably reduced, to 55.0±20.3% of control (n=29, Fig. 3c, Table 1), which suggests the ER as the source of the H_2O_2-evoked Ca^{2+} release. For confirmation, further drugs antagonizing Ca^{2+} release from the ER were applied. The ryanodine receptor antagonist dantrolene (20–40 µM, 8–15 min) decreased the H_2O_2-induced Ca^{2+} transients to 51.7±29.9% of control (n=59, Fig. 4a, e). Upon wash-out of dantrolene (20 min), the H_2O_2-elicited Ca^{2+} transients partially recovered (Table 1), which confirms that they were dampened by the antagonist and not as a consequence of lowered Ca^{2+} store content. Ryanodine applied in low concentrations (1 µM, 3–5 min) caused a moderate Ca^{2+} transient by itself (9.2±4.1%, n=7), which resembled the H_2O_2-induced effects, but it did not modulate the H_2O_2-evoked Ca^{2+} transient (106.0±22.3% of control, n=7). At higher concentrations (25 µM, 5–7 min), ryanodine itself did not induce any Ca^{2+} transients (n=7), but significantly depressed the H_2O_2-mediated Ca^{2+} release to 57.3±21.7% of control (n=12; Fig. 4e).

Since inhibition of ryanodine receptors only partly blocked the H_2O_2-mediated Ca^{2+} transients, we also tested for a possible involvement of IP3 receptors. Block of IP3 receptors by 2-APB (100 µM, 8–10 min) decreased the H_2O_2-induced Ca^{2+} transient to 46.9±27.7% of control (n=36, Fig. 4b, e), suggesting that IP3 receptors contribute to the H_2O_2-mediated Ca^{2+} release. Upon wash-out of 2-APB (10–20 min), the H_2O_2-mediated Ca^{2+} transients recovered, occasionally exceeding the magnitude of the control

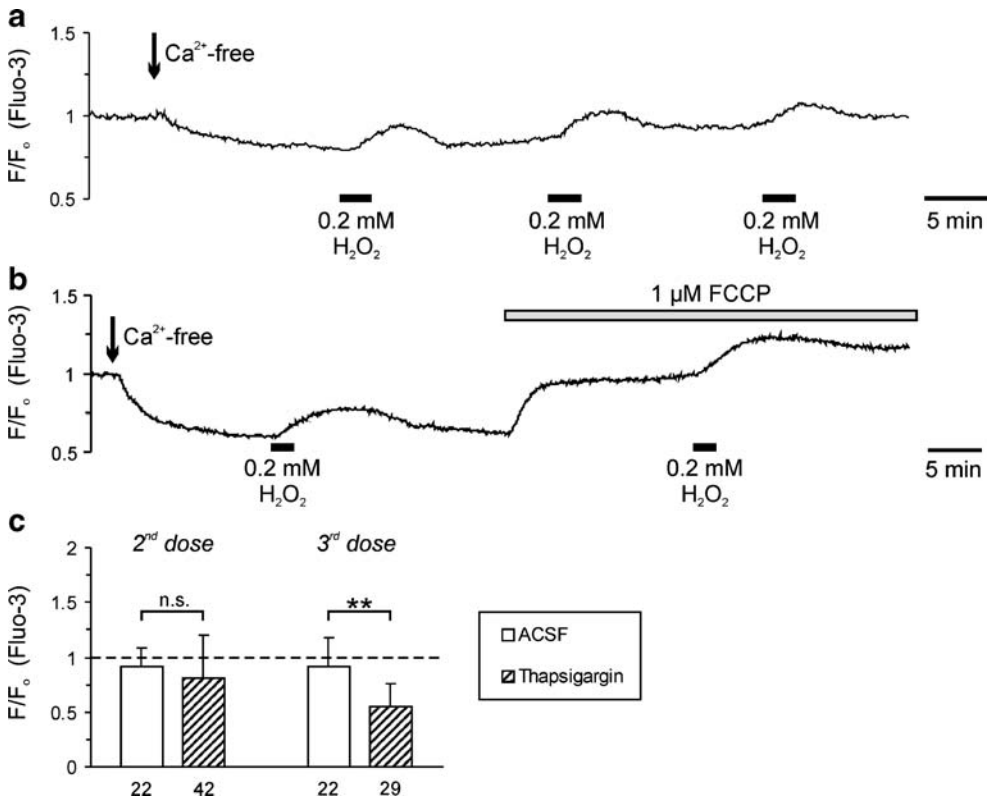

Fig. 3 The ER but not mitochondria are involved in the H_2O_2-induced Ca^{2+} transients. **a** Control experiments showed that despite withdrawal of extracellular Ca^{2+}, the H_2O_2-induced Ca^{2+} transients could be evoked repeatedly in cultured neurons without decreasing in amplitude. **b** The H_2O_2-mediated increase in $[Ca^{2+}]_i$ persisted upon mitochondrial uncoupling by FCCP, which indicates that mitochondria cannot be its source. **c** In the presence of thapsigargin (1 µM), the Ca^{2+} transients decreased when H_2O_2 was applied repeatedly

Table 1 Pharmacological properties of the H_2O_2-induced Ca^{2+} transients in cultured hippocampal neurons

Treatment	2nd dose H_2O_2 (200μM)	3rd dose H_2O_2 (200μM)
Control (Ca^{2+}-free ACSF)	91.8±17.2% (*n*=22)	91.0±26.6% (*n*=22)
FCCP (1 μM)	81.4±34.1% (*n*=32)	n.d.
Thapsigargin (1 μM)	81.5±38.9% (*n*=42)	55.0±20.3%** (*n*=29)
Dantrolene (20–40 μM)	51.7±29.9%** (*n*=59)	71.7±39.7%* (*n*=44)
Ryanodine (25 μM)	57.3±21.7%** (*n*=12)	n.d.
2-APB (100 μM)	46.9±27.7%** (*n*=36)	122.0±71.6% (*n*=36)
2-APB + dantrolene (100+40 μM)	28.4±15.7%** (*n*=32)	104.1±47.1% (*n*=32)

Reported is the relative amplitude of the H_2O_2-evoked Ca^{2+} transients (monitored as increases in fluo-3 fluorescence) in Ca^{2+}-free solutions and the presence of various drugs. All Ca^{2+} changes are normalized to the respective control responses to H_2O_2 (200 μM) recorded previously in each cell in Ca^{2+}-free control solutions. Also, for comparison, the *upper row* contains the responses to repetitive H_2O_2 administration in control solutions. Significance of the drug-induced changes was tested in unpaired *t* tests, comparing the average amplitudes observed in the presence of drugs to the second H_2O_2 dose under control conditions and the changes observed upon wash-out of the drugs to the third H_2O_2 dose under control conditions

n.d. not determined

*$P<0.05$; **$P<0.01$

responses (Fig. 4b and Table 1). Combined inhibition of ryanodine and IP3 receptors efficiently depressed the H_2O_2-induced Ca^{2+} release (reversible depression to 28.4±15.7% of control, *n*=32; Fig. 4c, e; Table 1).

To confirm that the H_2O_2-mediated Ca^{2+} release involves oxidation of SH groups, cultured cells were pretreated with DTT (2 mM, 5 min), a compound protecting exposed SH groups by keeping them in the reduced state [12, 34]. In the presence of DTT, the H_2O_2 (200 μM, 2–3 min)-induced Ca^{2+} rise was markedly depressed to 34.3±19.5% of its control amplitude, and upon 15-20 min wash-out of DTT it recovered to 80.0±49.8 % of control (*n*=13, Fig. 4d, e).

Furthermore, we tested for the putative involvement of other ROS. In the presence of Fe^{2+}, H_2O_2 may react in a Fenton reaction to hydroxyl radicals [14, 35]. To elucidate whether hydroxyl radicals contribute to the Ca^{2+} release, we blocked the Fenton reaction with the iron chelator deferoxamine mesylate (500 μM, 10–12 min pretreatment before H_2O_2 was added). As a result, the H_2O_2-mediated Ca^{2+} transient increased to 187±58% of control (*n*=6, Fig. 4e), suggesting that some of the administered H_2O_2 had indeed been converted to hydroxyl radicals. Application of $FeSO_4$ (500 μM, 5 min pretreatment), which forces the generation of hydroxyl radicals upon H_2O_2 administration, reduced the Ca^{2+} transient to 56.0±25.2% of control (*n*=19, Fig. 4e). This suggests that H_2O_2 itself, but not its secondary conversion into hydroxyl radicals, released Ca^{2+} from the ER. In addition, we tested whether superoxide affects $[Ca^{2+}]_i$. Application of xanthine (25 μM) plus xanthine oxidase (12.5 mU/ml), an established method to generate extracellular superoxide [7], increased fluo-3 emission despite the absence of extracellular Ca^{2+} by 191.7±35.0% (*n*=19, Fig. 5a). In the presence of the superoxide-dismutase inhibitor DEDTC (10 mM, 7 min pretreatment) the superoxide-induced Ca^{2+} transients were reduced to 63.6±10.1% of their control magnitude, and upon 5–10 min wash-out of DEDTC, they recovered to 85.1±18.8% of control (*n*=19). This partial depression by DEDTC suggests that the superoxide itself as well as its secondary conversion to H_2O_2 may have contributed to the Ca^{2+} transients.

Next, we asked whether endogenous generation of ROS would be sufficient to release Ca^{2+} from the ER. For that purpose, we provoked an imbalance of cytosolic ROS generation and elimination by blocking the H_2O_2 cleaving enzyme glutathione peroxidase with MCS, a treatment leading to cytosolic H_2O_2 accumulation [4]. Applied in Ca^{2+} free solutions, MCS (5 mM, 3–5 min) increased fluo-3 emission by 29.6±18.9% (*n*=11). In the presence of dantrolene (20 μM, 6–8 min pretreatment), the MCS-induced Ca^{2+} rise was severely decreased to 17.8±7.6% of its control amplitude (Fig. 5b), confirming Ca^{2+} release from the ER. Upon wash-out of dantrolene (15–20 min), the MCS-induced Ca^{2+} rise partially recovered to 40.3±27.8% of control (*n*=11, Fig. 5b).

Modulation of second messenger mediated Ca^{2+} release by H_2O_2

After having successfully demonstrated that both extracellularly applied and endogenously generated H_2O_2 may release Ca^{2+} from the ER, we were curious whether oxidative modulation of the Ca^{2+} content of the ER affects neuronal Ca^{2+} signaling in response to, e.g., activation of

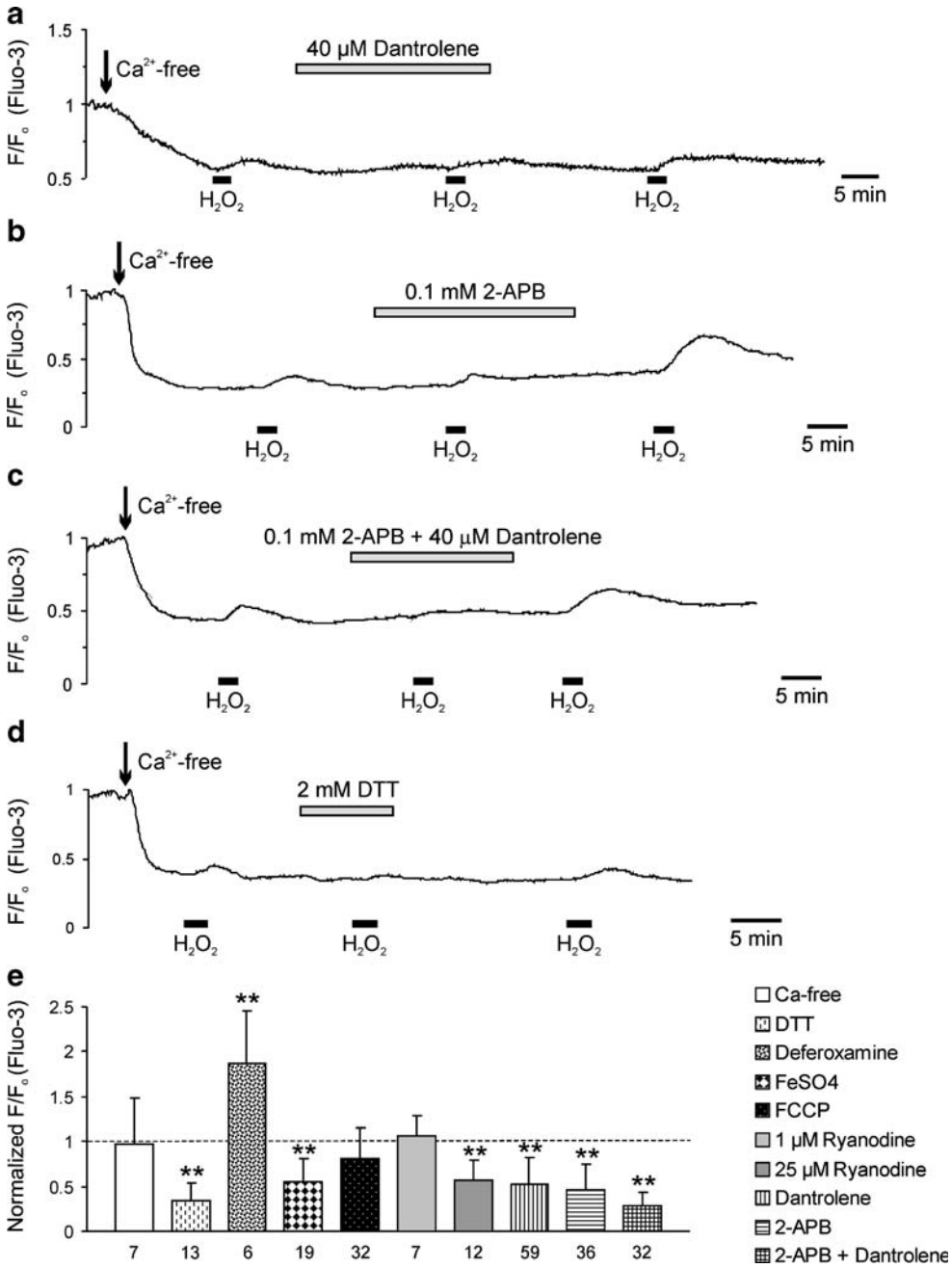

Fig. 4 H_2O_2 releases Ca^{2+} from the ER via ryanodine and IP3 receptors. **a** The ryanodine receptor antagonist dantrolene markedly decreased the amplitude of the H_2O_2-induced Ca^{2+} rise, and upon wash-out of dantrolene the Ca^{2+} transients recovered. In all displayed traces, H_2O_2 was consistently applied at a concentration of 200 μM. **b** The IP3 receptor antagonist 2-APB also reversibly depressed the H_2O_2-induced Ca^{2+} rise. **c** Combined inhibition of both ryanodine and IP3 receptors almost abolished the H_2O_2-induced Ca^{2+} rise in a reversible manner. **d** The sulfhydryl (SH)-protectant dithiothreitol (*DTT*) severely depressed the H_2O_2-induced Ca^{2+} release, confirming that H_2O_2 indeed acts via oxidative modulation of SH groups. **e** Summarized pharmacological profile of the H_2O_2 (200 μM)-induced Ca^{2+} transients. Each drug targeting the ER, ryanodine, or IP3 receptors clearly reduced the H_2O_2-induced Ca^{2+} rise. All drugs, except for deferoxamine and $FeSO_4$, were applied in Ca^{2+}-free solutions. Plotted are the normalized Ca^{2+} responses, referred to the control responses evoked by H_2O_2 in each cell before drug treatment. *Asterisks* mark statistically significant changes (**$P<0.01$), as compared to the second application of H_2O_2 recorded in untreated control cells (see: Fig. 3a, c)

PLC-coupled metabotropic receptors. We therefore applied the purinergic P2Y receptor agonist UTP (100 μM, 2–3 min) [46] or glutamate (30 μM, 2-3 min) in Ca^{2+}-free solutions and observed an increase in fluo-3 fluorescence by 13.7±6.1% (n=17; Fig. 6a) and 32.4±20.7% (n=15; Fig. 6b), respectively. Pretreatment with H_2O_2 (200 μM, at least 2 min) reversibly depressed the UTP and the glutamate-induced Ca^{2+} release to 25.3±24.5% (n=17) and 32.4±20.7% (n=15) of control, respectively (Fig. 6). This confirms that oxidative conditions mediated by increased H_2O_2 levels are indeed capable of modulating the efficacy of PLC-mediated signaling.

Modulation of mitochondrial function by H_2O_2

Mitochondrial function and structure may be potentially impaired by oxidative stress, resulting in disturbed ATP supply and induction of the mitochondrial permeability transition—as has been reported for chronic administration of H_2O_2 (50 μM, up to 48 h) in cell cultures [11]. Therefore, we determined to what degree acute administration of H_2O_2 modulates mitochondrial function, i.e., $\Delta\Psi_m$, NADH/FAD autofluorescence, mitochondrial structure, and cellular ATP content. Changes in $\Delta\Psi_m$ were monitored by imaging Rh123 fluorescence [18, 19]. Accumulation of

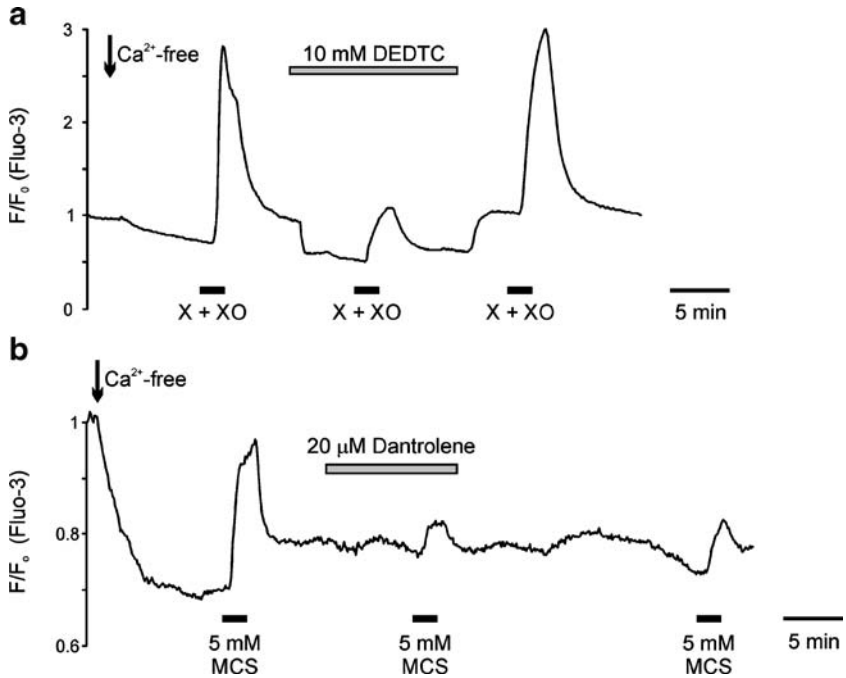

Fig. 5 Extracellular generation of superoxide and accumulation of endogenously generated H_2O_2 also releases Ca^{2+} from intracellular stores. **a** Extracellular generation of superoxide by combined administration of xanthine (*X*, 25 μM) and xanthine oxidase (*XO*, 12.5 mU/ml) induces an increase in $[Ca^{2+}]_i$ in cultured neurons that is more variable and intense than the H_2O_2-induced Ca^{2+} rise. The superoxide dismutase inhibitor DEDTC markedly depressed this Ca^{2+} rise, suggesting that both superoxide and secondarily generated H_2O_2 contributed to the intracellular release of Ca^{2+}. The sudden drop in fluo-3 emission upon DEDTC application is due to competitive absorption of DEDTC. Upon wash-out of DEDTC, the Ca^{2+} transient fully recovered to its original amplitude. **b** Forcing the cytosolic accumulation of endogenously generated H_2O_2 in cultured neurons by inhibiting the H_2O_2 scavenging enzyme glutathione peroxidase with mercaptosuccinic acid (*MCS*) also released Ca^{2+} from intracellular stores in a dantrolene-sensitive manner

Rh123 in functional mitochondria increasingly diminishes its fluorescence due to self quenching. Upon mitochondrial depolarization, some Rh123 is released into the cytosol, where—due to dequenching—its fluorescence emission increases again [18, 19]. Accordingly, mitochondrial depolarization is reported as an increase in cellular Rh123 fluorescence. Changes in Rh123 fluorescence were quantified in a small (40×60 μm) region of interest in *st. radiatum* of the CA1 subfield. As reference signals, the maximum depolarization evoked by the mitochondrial uncoupler FCCP as well as the mitochondrial depolarization in response to respiratory chain blockade by CN^- were determined.

In adult slices (isolated hippocampal formation, bulk loaded with 4–5 μg/ml Rh123 for 25–30 min), mitochondrial uncoupling by FCCP (1 μM, 5 min) and block of mitochondrial respiration by CN^- (1 mM, 5 min) increased Rh123 fluorescence by 117.5±18.7% (n=7) and 46.5±6.9% (n=6), respectively (Fig. 7a, c). In comparison, H_2O_2 exerted only moderate effects; 200 μM and 1 mM H_2O_2 (5 min) hardly affected Rh123 fluorescence, 1.0±1.4% and 3.5±4.1%, respectively. Applied at a concentration of 5 mM, H_2O_2 increased Rh123 fluorescence by 6.1±3.2% (n=6 each, Fig. 7a, c), i.e., on average it increased Rh123 fluorescence by only 5.2% of the maximum response determined by mitochondrial uncoupling. To estimate to what degree the efficiency of H_2O_2 may be restricted in tissue slices by diffusional limitations and cleavage by cellular self-defense systems such as catalase and glutathione peroxidase [16], we also quantified the effects of H_2O_2 on $\Delta\Psi_m$ in cultured neurons and obtained somewhat more intense responses. FCCP (1 μM, 2–3 min) and CN^- (1 mM, 2–3 min) increased Rh123 fluorescence by 49.1±35.8% (n=134) and 16.6±11.2% (n=66), respectively, whereas application of 0.2, 1, and 5 mM H_2O_2 (2 min) increased Rh123 fluorescence by 15.9±10.9% (n=82), 20.7±13.9% (n=12), and 24.3±18.8% (n=14, Fig. 7c), i.e., on average by no more than 32.4% of the maximum response seen upon mitochondrial uncoupling. That CN^- induced somewhat more moderate effects in cultured cells obtained from neonatal rats (34% of the FCCP response) than in acute slices obtained from adult rats (40% of the FCCP response) could be shown to resemble an age-dependent effect. Applied to acute tissue slices of juvenile rats (p13–15), CN^- increased Rh123 fluorescence by 30.9±3.5% (n=8, data not shown), i.e., on average by 29% of the response evoked by FCCP (106.8±5.8%, n=5), which is similar to the effects observed in cultured cells.

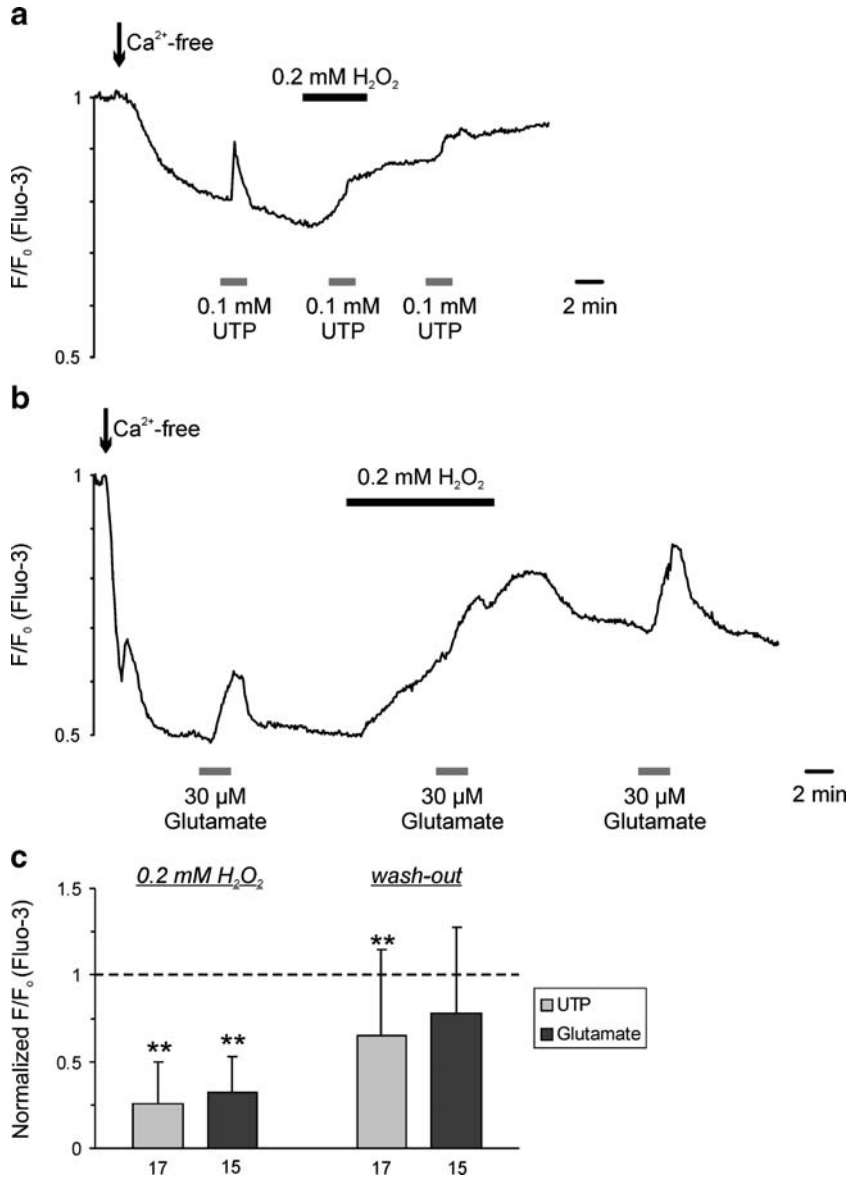

Fig. 6 Phospholipase C (PLC)-mediated Ca^{2+} signaling in cultured neurons is dampened by H_2O_2. **a** The purinergic P2Y receptor agonist uridine-5′-trisphosphate (UTP, 100 µM) induced moderate Ca^{2+} transients which were markedly depressed in the presence of H_2O_2 and recovered upon wash-out. Note that upon the prolonged application of H_2O_2 the Ca^{2+} baseline remained elevated. **b** The Ca^{2+} responses evoked by metabotropic glutamate receptor stimulation (glutamate applied in Ca^{2+}-free solutions) were also largely reduced in the presence of H_2O_2. **c** Statistical summary showing the dampening of PLC-mediated Ca^{2+} signaling during H_2O_2-mediated oxidative conditions and their recovery upon wash-out of H_2O_2. *Asterisks* mark significant changes as compared to the previously recorded control responses (**$P<0.01$)

In Ca^{2+}-free solutions containing dantrolene (20 µM), the H_2O_2 (200 µM)-mediated increase in Rh123 fluorescence in cultured cells was decreased to 47.8±35.5% of the response seen without dantrolene in each neuron (n=17), suggesting that—at least in part—the mitochondrial depolarization is due to the mitochondrial uptake of Ca^{2+} previously released from the ER, rather than a direct effect of H_2O_2 on $\Delta\Psi_m$.

To obtain a direct measure of changes in mitochondrial metabolism, i.e., oxidative phosphorylation, we also monitored NADH and FAD autofluorescence [17, 19, 22] and quantified its changes in a small region of interest (~40×60 µm) within *st. radiatum* of the CA1 subfield. In acute hippocampal slices (adult rats), 0.2, 1, and 5 mM H_2O_2 (5 min) caused only moderate changes in tissue autofluorescence; NADH fluorescence decreased by 2.6±1.2% (n=5), 4.8±5.8% (n=6), and 12.3±1.9% (n=6), respectively, indicating oxidation of NADH to NAD^+. FAD fluorescence showed the opposite changes in response to 0.2, 1, and 5 mM H_2O_2, increasing by 2.5±1.6% (n=6), 2.6±1.0% (n=6), and 7.0±1.7% (n=6), respectively, which indicates oxidation of $FADH_2$ to FAD (Fig. 7b, c). In comparison, arrest of mitochondrial respiration by 1 mM CN^- caused a 12.2±5.1% (n=6) increase in NADH fluorescence (reduction of NAD^+ to NADH) and a 5.3±2.2% decrease in FAD fluorescence (reduction of FAD to $FADH_2$; n=6, Fig. 7b, c). Mitochondrial uncoupling by 1 µM FCCP decreased NADH fluorescence by 14.7±1.5% and increased FAD fluorescence by 2.2±1.5% (n=8 each), which corresponds to earlier observations [22]. In cultured hippocampal neurons, only changes in NADH autofluorescence were determined (excitation 363 nm, 400-nm beam-splitter,

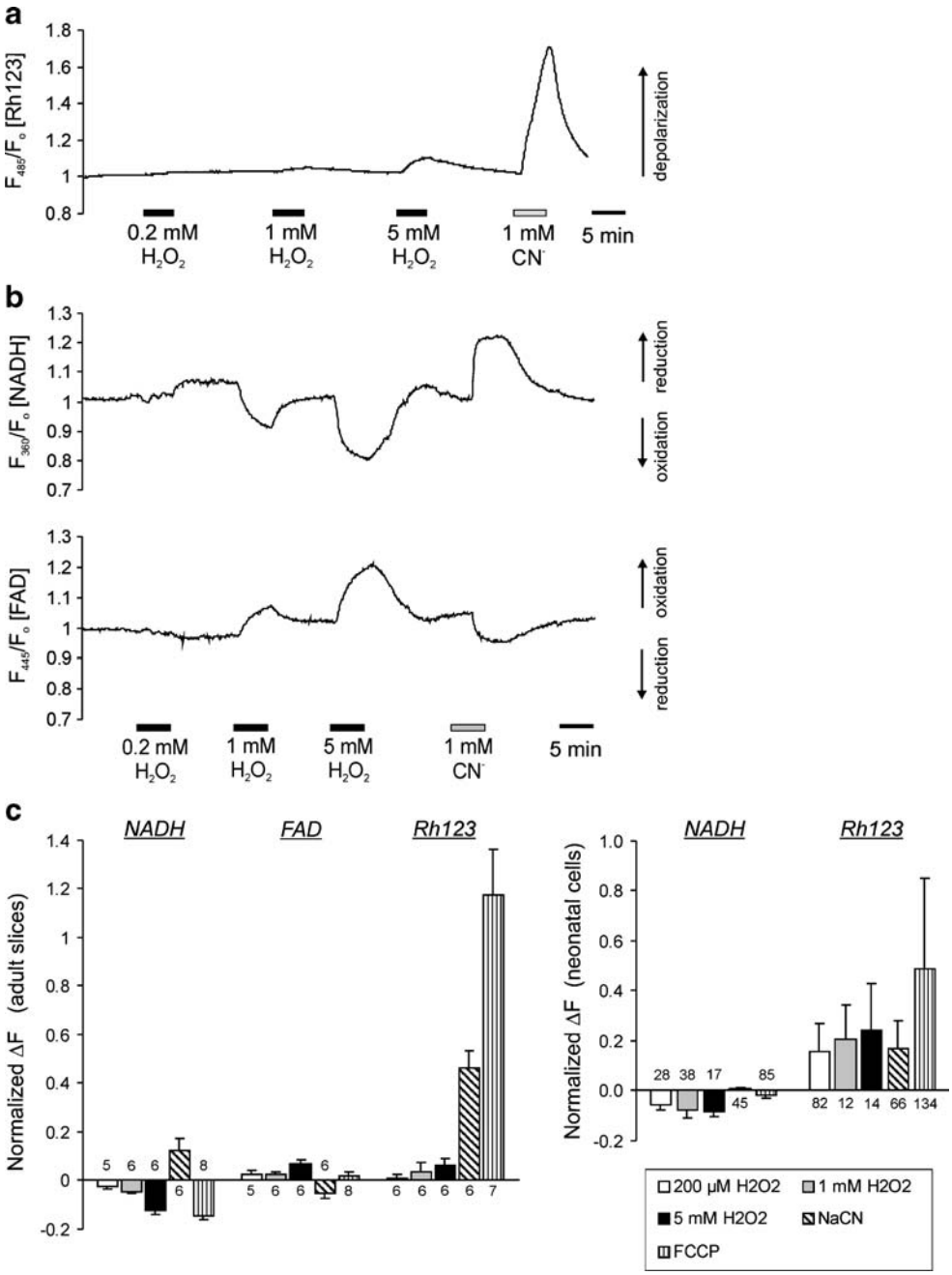

Fig. 7 Mitochondrial function is only moderately affected by H_2O_2. **a** Mitochondrial membrane potential, as probed by changes in Rh123 fluorescence in acute hippocampal tissue slices of adult rats, decreases only slightly in response to H_2O_2. For comparison, the massive mitochondrial depolarization in response to inhibition of complex IV of the mitochondrial respiratory chain by CN^- (applied as NaCN) is shown. **b** Combined recordings of NADH and FAD autofluorescence in acute tissue slices show the expected increase in NADH and decrease in FAD levels upon block of mitochondrial metabolism by CN^-. In comparison, H_2O_2 decreased NADH levels (oxidation of NADH) and increased FAD levels (oxidation of $FADH_2$), which apparently reflects direct oxidation of NADH and $FADH_2$ by H_2O_2. **c** Summary of the effects of H_2O_2 on mitochondrial membrane potential (Rh123 fluorescence) as well as mitochondrial metabolism (cellular NADH and FAD levels). Note the opposite effects of H_2O_2 and CN^- on NADH and FAD levels, but the equally directed responses in Rh123 fluorescence

447/60-nm bandpass filter as emitter), because FAD fluorescence was too weak to be monitored reliably. Application of 0.2, 1, and 5 mM H_2O_2 (2 min) moderately decreased NADH autofluorescence by 5.8±2.1% (n=28), 7.7±3.2% (n=38), and 8.2±2.1% (n=17), respectively. Application of 1 mM CN^- and 1 µM FCCP hardly affected NADH fluorescence (increase by 0.7±0.7%, n=45 and decrease by 2.1±0.9%, n=85, respectively, Fig. 7c).

Quantifying cellular ATP content in acute adult hippocampal tissue slices revealed that H_2O_2 somewhat decreased ATP levels. Control slices contained 11.4±3.8 nmol ATP/mg protein (n=22), and those exposed to H_2O_2 (5 mM, 20 min) contained 8.2±2.0 nmol ATP/mg protein (n=6), i.e., 72% of the ATP level of untreated slices. As reported earlier, treatment with 1 mM CN^- (chemical anoxia, 20 min) depleted cellular ATP (0.2±0.3 nmol ATP/mg protein, n=6) [22].

Metabolic and excitotoxic insults are capable of disturbing the subcellular organization of mitochondria [37, 47, 54]. To screen for such changes, we prolonged the application of H_2O_2 to ensure capturing of any changes, because effects on mitochondrial positioning or intracellular trafficking develop only after several minutes. Multiphoton imaging of individual Rh123-labeled mitochondria [37, 38] in cultured hippocampal neurons revealed that mitochondrial structure and subcellular distribution were not disturbed by administration

of 1-5 mM H_2O_2 for up to 15 min (n=4, Fig. 8). Yet, as obvious from the Supplemental movie and the kymographic plots (Fig. 8b), which report the spatial positions of the single mitochondrial structures over time, the directed movements of mitochondria were halted in the presence of H_2O_2 within 3–5 min. In Ca^{2+}-free solutions containing 20 µM dantrolene, H_2O_2 (200 µM, up to 10 min) still arrested mitochondrial movements (n=10). This indicates

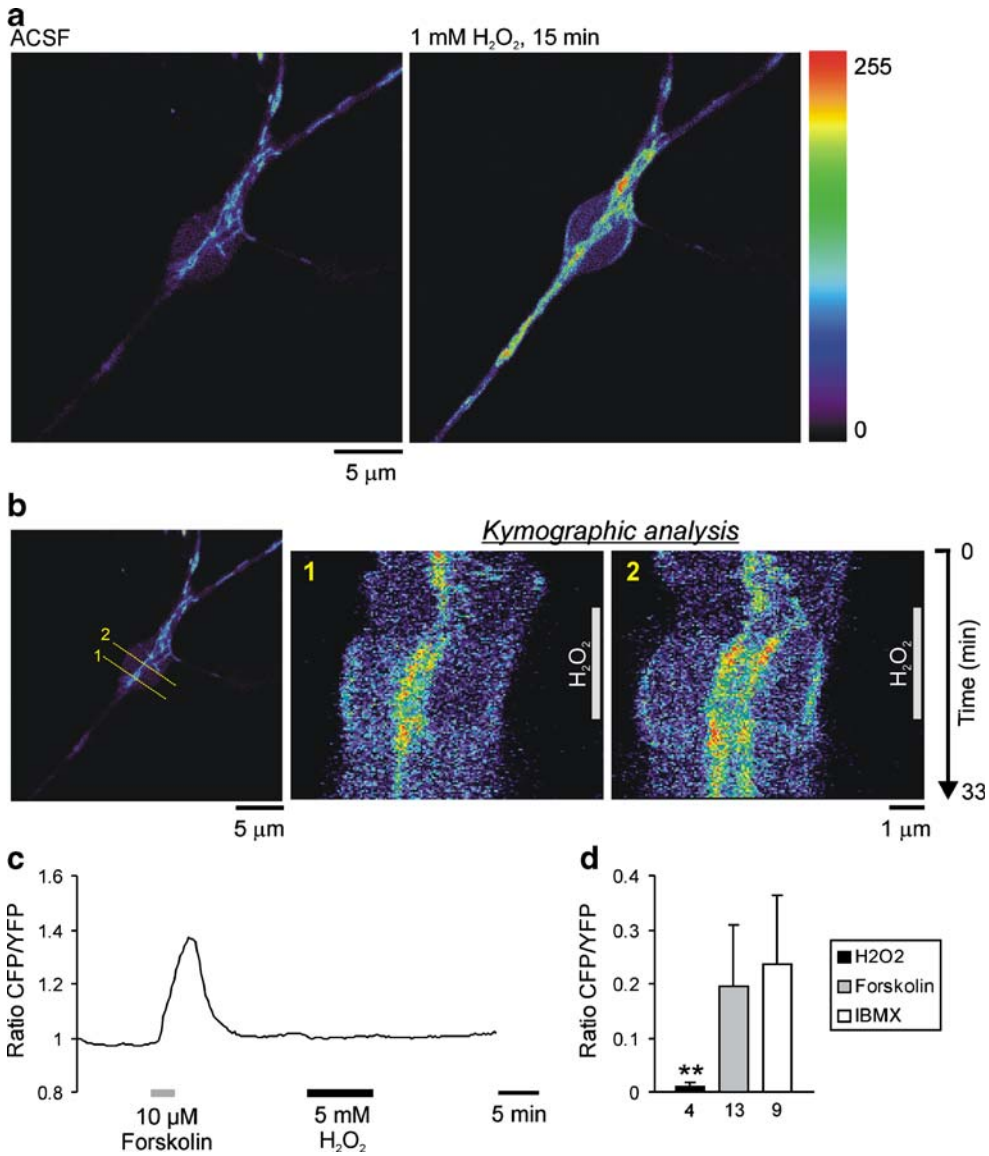

Fig. 8 H_2O_2 arrests the intracellular trafficking of mitochondria. **a** Applied to cultured hippocampal neurons for 15 min, H_2O_2 depolarized mitochondria—as indicated by the increase in Rh123 fluorescence—but did not de-arrange their subcellular distribution. As can be seen from the Supplemental movie, the intracellular trafficking of mitochondria was halted in the presence of 1 mM H_2O_2. Mitochondria were visualized using a custom-built two-photon laser scanning microscope and a ×63 infrared optimized objective (Zeiss IR-Achroplan); pixel resolution was 125 nm/pixel. Mitochondria were labeled by Rh123 loading (3–5 µg/ml, 25–30 min). **b** Kymographic analysis performed at the two indicated lines of interest (*1*, *2*) visualizes the movement of mitochondria and its arrest by H_2O_2. In the resulting kymographic plots, the pixel intensities along the line of interest are plotted versus time. Pixel intensities in the first image of the series yield the top line of the kymographic plot (time zero), pixel intensities of the second image the second line of the plot, and so on. In the resulting plots, left/right shifting of structures, i.e., variability among neighboring lines, indicates mitochondrial movement, whereas no shifting (no variability between lines) indicates resting mitochondria. Note that in the presence of 1 mM H_2O_2 (indicated by the *white bar* in each kymographic plot), the motility of mitochondria was minimized. **c**, **d** As probed with a genetically encoded cAMP-sensitive FRET construct in cultured hippocampal neurons, H_2O_2 does not affect the cytosolic cAMP level. Plotted is the intensity ratio of CFP/YFP fluorescence. Forskolin and IBMX clearly increased the CFP/YFP ratio (decreased FRET efficiency), which corresponds to a rise in cytosolic cAMP levels. In contrast, administration of H_2O_2 did not affect the CFP/YFP ratio. *Asterisks* mark significant changes (**P<0.01) as compared to the effects of IBMX and forskolin

that H_2O_2-mediated oxidative conditions modulate the intracellular trafficking of mitochondria and that Ca^{2+} release from the ER is not the primary cause for the arrest of mitochondrial movements.

Previously, we have reported for cultured brainstem neurons that an arrest of mitochondrial trafficking may occur in response to increased intracellular cAMP levels [37]. Using a genetically encoded cAMP-sensitive FRET construct [44, 49] and an optical image-splitter device, we therefore elucidated whether H_2O_2 modulates cytosolic cAMP levels. Expressed in hippocampal neurons, the CFP/YFP FRET construct reliably reports changes in cytosolic cAMP. Stimulation of adenylate cyclase with forskolin (10 μM, 3 min) or inhibition of phosphodiesterase with IBMX (500 μM, 5 min) increased the CFP/YFP fluorescence ratio (donor/acceptor ratio) by 19.5±11.3% (n=13) and 23.5±12.9% (n=9), respectively. However, no changes in the CFP/YFP ratio were observed upon administration of H_2O_2 (5 mM, 5–7 min, n=4; Fig. 8c, d).

Discussion

We probed for the effects of externally applied H_2O_2, i.e., the consequences of an acute oxidative shift in cytosolic redox state within the hippocampal network. Focusing on the modulation of cytosolic signaling as well as organelle function and interaction, we found that H_2O_2 induced the release of Ca^{2+} from the ER and dampened PLC-coupled metabotropic signaling, but only slightly modulated $\Delta\Psi_m$ and mitochondrial metabolism. The relative levels of the cytosolic redox couples NAD/NADH and FAD/$FADH_2$ were shifted towards more oxidized conditions. The intracellular cAMP level was not affected by H_2O_2, indicating that the halting of mitochondrial trafficking occurred in a cAMP-independent manner.

Modulation of intracellular Ca^{2+} stores by H_2O_2

H_2O_2 (200 μM) released Ca^{2+} from intracellular stores, and only at the highest concentration tested (5 mM H_2O_2), Ca^{2+} influx from the extracellular space contributed slightly. The H_2O_2-mediated Ca^{2+} rise persisted in the presence of the mitochondrial uncoupler FCCP, but was antagonized by thapsigargin, 2-APB, dantrolene, and high concentrations of ryanodine (25 μM). The dose-dependent effect of ryanodine arises from the fact that low concentrations (nanomolar range) promote Ca^{2+}-permeable (conducting) sublevel states of the ryanodine receptor, whereas higher micromolar levels lock the receptor in the closed (non-conducting) state [55]. Since the H_2O_2-mediated Ca^{2+} response was not potentiated by "agonistic" low doses of ryanodine, these two modes of receptor activation do not seem to be additive. In view of this pharmacological profile, we conclude that H_2O_2 mediates the activation of both ryanodine as well as IP3 receptors which identifies these receptors as redox-sensitive targets in hippocampal neurons being potentially activated by oxidizing conditions. Extracellular generation of superoxide also released Ca^{2+} from the ER, whereas a contribution of hydroxyl radicals can be excluded.

A similar intracellular Ca^{2+} release was reported for cultured rat hippocampal astrocytes, in which mitochondria and ER released Ca^{2+} in response to 100 μM H_2O_2 [23]. Interestingly, ryanodine as well as IP3 receptors have been reported to be redox-sensitive. Their redox-sensing elements are hyper-reactive SH groups, whose redox potential critically affects channel gating [3, 56, 60, 61]. Compounds mediating SH reduction decrease, whereas those promoting SH oxidation increase ryanodine receptor activity [28, 63]. Accordingly, on the subcellular level, oxidative activation of these receptors and the resulting release of Ca^{2+} may give rise to the formation of cytosolic Ca^{2+} microdomains as was demonstrated in cardiomyocytes [13]. Also their oxidation has been found to induce hippocampal long-term potentiation in response to increased superoxide formation [30]. Likewise, in spinal cord inhibitory interneurons as well as umbilical vein endothelial cells, H_2O_2 was reported to release Ca^{2+} from IP3-controlled intracellular stores [56, 61]. That the H_2O_2-induced release of Ca^{2+} from the ER in hippocampal neurons also involves oxidation of SH-groups is indicated by the antagonistic effect of the SH-protectant DTT.

In most experiments, we applied H_2O_2 extracellularly, but accumulation of endogenously generated H_2O_2 was equally capable of releasing Ca^{2+} from the ER. This confirms the physiological relevance of the oxidative modulation of ryanodine and IP3 receptors. Furthermore, an interaction of H_2O_2-mediated oxidative conditions was verified for metabotropic signaling via glutamate and purinergic P2Y receptors. The signaling efficacy of both receptors was dampened in the presence of H_2O_2—obviously by converging the effects on Ca^{2+} release from the ER. Accordingly, the unveiled oxidative modulation of ryanodine and IP3 receptors could contribute to the adaptation of neuronal responsiveness and metabotropic signaling to cytosolic redox conditions and mitochondrial activity.

In this context, an interesting future aspect could be whether dysfunction of single mitochondria would be efficient to generate localized ROS microdomains, thereby triggering highly localized Ca^{2+} release from nearby ER segments. Analysis of such localized events requires optical tools allowing for the visualization of compartment-specific ROS microdomains. At present, the limitations of commercially available redox-sensitive dyes (irreversible oxidation and sensitivity to autooxidation) prevent, however, reliable imaging of ROS microdomain dynamics (see also discussion in [19]).

Mitochondria as targets for oxidative modulation

The H_2O_2-induced changes in cellular autofluorescence indicate direct oxidation of NADH and $FADH_2$. Mitochondria-mediated oxidation of these electron donors would require intensified mitochondrial respiration, yet the somewhat increased Rh123 fluorescence reports mitochondrial depolarization, i.e., slightly reduced respiratory activity in the presence of H_2O_2. Furthermore, in part, the H_2O_2-mediated depolarization of mitochondria was shown to be due to the mitochondrial uptake of Ca^{2+} previously released from the ER. That the H_2O_2-mediated mitochondrial depolarization was more pronounced in cultured cells than in slices may be due to diffusional limitations and/or partial breakdown of H_2O_2 within the tissue by cellular self-defense systems such as astrocytic catalase and neuronal glutathione peroxidase [15, 16]. Nevertheless, as compared to the complete mitochondrial depolarization upon FCCP application, even 5 mM H_2O_2 caused an only partial depolarization. These rather moderate $\Delta\Psi_m$ responses to H_2O_2 are in line with an earlier study on cultured rat forebrain neurons [29], where a prominent increase in Rh123 fluorescence was only seen when higher concentrations of H_2O_2 (10–30 mM) were applied for several minutes. The fact that the CN^--mediated effects on cellular NADH levels and $\Delta\Psi_m$ were more pronounced in slices than in cell cultures arises from the different level of maturation [6, 19, 31]. Cell cultures were obtained from neonatal rats (postnatal days 2–4), whereas the acute slices were prepared from adult rats (4–6 weeks). The control experiments performed on juvenile slices show similar CN^- effects on Rh123 fluorescence as seen in cell cultures. Also, it should be kept in mind that the tissue responses in slices constitute an integrated signal of neurons and a certain contribution of glial cells, whereas in cell cultures, purely neuronal signals are recorded. Nevertheless, the tissue signals can be assumed to be dominated by neuronal responses because neurons are more vulnerable to metabolic insults than glial cells [50] and contain a higher mitochondrial density [45]. Also, in our earlier experiments [26], comparing the various layers of the CA1 subfield (*st. oriens*, *st. radiatum*, *st. pyramidale*) yielded identical responses in NADH/FAD autofluorescence upon CN^- treatment and Rh123 fluorescence upon mitochondrial uncoupling, even though the glial cell density differs among these layers, as others have shown by immunolabeling for glial acidic fibrillary protein [62].

Higher levels of H_2O_2 (5 mM) somewhat decreased the cellular ATP content of hippocampal slices, another indication for less intense mitochondrial respiration. However, a marked negative impact of the moderate mitochondrial depolarization and the ~28% lower cellular ATP content on hippocampal network activity and function seems unlikely. As we reported earlier, the tolerance of acute hippocampal slices to severe hypoxia was improved in the presence of H_2O_2 [26, 27], and the fact that HSD episodes could still be induced upon 20–25 min pretreatment of slices with 5 mM H_2O_2 confirms the viability of the tissue.

Application of H_2O_2 halted the intracellular trafficking of mitochondria (Supplemental movie). Mitochondrial trafficking is an energy-demanding transport along microtubules which involves molecular motors and is modulated by cAMP-mediated protein phosphorylation [37]. The H_2O_2-mediated halting of mitochondrial trafficking suggests that the subcellular distribution of mitochondria may as well be regulated by cytosolic redox changes. With H_2O_2 being a by-product of mitochondrial respiration [8], such "autoregulation" could help to ensure that mitochondria are immobilized at locations with optimized O_2 supply. Since H_2O_2 did not affect intracellular cAMP levels, protein phosphorylation downstream of cAMP—which halts mitochondrial trafficking in cultured brainstem neurons [37]—does not seem to contribute to the H_2O_2-mediated arrest of mitochondrial transport. The moderate Ca^{2+} transient induced by H_2O_2 seems also unlikely as a cause, because mitochondrial trafficking was also blocked in Ca^{2+}-free solutions containing dantrolene. Since mitochondrial transport is energy demanding and can also be antagonized by metabolic disturbances [37], the observed halting of mitochondrial trafficking may arise from the H_2O_2-mediated moderate decrease in cellular ATP content. Also, molecular motors may constitute an oxidation-sensitive target, a possibility that needs to be analyzed in further experiments.

Acute versus chronic effects of H_2O_2

Whereas we have investigated the effects of acute H_2O_2 application, others have found that the continued application of even low levels of H_2O_2 mediates apoptotic cell death in a mouse beta-cell line (MIN6N8a). In these cells, H_2O_2 released Ca^{2+} from the ER via ryanodine and IP_3 receptors, which—during application of 50 μM H_2O_2 for up to 24 h—led to pronounced apoptotic cell loss, with cytochrome c being released from mitochondria after 6 h of H_2O_2 treatment [11]. Direct H_2O_2-mediated mitochondrial damage or energy depletion, however, does not seem to be involved in MIN6N8a cell death. The intracellular Ca^{2+} rise rather seems to activate a variety of Ca^{2+}-sensitive enzymes and stress kinases, which then trigger the mitochondrial permeability transition, followed by cytochrome c release and caspase activation [11]. Nevertheless, H_2O_2 was reported to severely deplete cellular ATP in cell cultures, and hippocampal neurons were more vulnerable than cortical neurons or immortalized hippocampal HT22 cells [57]. In cultured hippocampal neurons, application of 0.8 mM H_2O_2 (10 min) decreased cellular ATP levels to 5% of the control level and ATP decline started already after 1 min of H_2O_2 treatment [57]. A marked methodological difference is, however, that

these cultures were obtained from fetal rats (E18), whereas we prepared cell cultures from neonatal rats. Also in these embryonic tissue-based cultures, a marked drop in ATP content was already evident under baseline control conditions in solutions containing normal Ca^{2+} content [57].

Concluding remarks

An acute H_2O_2-mediated oxidative shift in the intracellular redox state induced a variety of effects in single hippocampal neurons and within the hippocampal network. These include modulation of intracellular signaling cascades and neuronal excitability, targeting of mitochondrial polarization and as such energy supply, and the halting of subcellular mitochondrial trafficking. In view of cytosolic signaling especially the modulation of intracellular Ca^{2+} stores clearly is of importance for the adaptation of neuronal responsiveness and network activity to cytosolic redox state and metabolic supply. The level of intracellular Ca^{2+}—a ubiquitous second messenger—seems to be linked to changes in cellular redox state, with oxidative conditions mediating the release of Ca^{2+} within defined cellular compartments. This can already be achieved by low concentrations of H_2O_2, which—as demonstrated by others—do not even exert noticeable effects on synaptic function [20, 41, 43]. Accordingly, ROS released by respiring mitochondria may act as cytosolic messengers involved in organelle–organelle interactions—especially the mitochondria–ER crosstalk. As a consequence, the efficacy of metabotropic PLC-mediated signaling cascades is modified. In view of the membrane permeability of H_2O_2, one may even speculate that H_2O_2 does not only act at its generation site, but may also modulate neighboring neurons and glial cells.

Acknowledgments We are grateful to Dr. Kees Jalink (The Netherlands Cancer Institute) for providing us with the cAMP-sensitive FRET construct (CFP-Epac-(delta-DEP, CD)Venus). Also, we are grateful to Prof. Irmelin Probst for her help with the determination of cellular ATP levels. This study was supported by the Deutsche Forschungsgemeinschaft (EXC 171 and CMPB) and Göttingen University (Ausstattungsmittel Juniorprofessur).

Open Access This article is distributed under the terms of the Creative Commons Attribution Noncommercial License which permits any noncommercial use, distribution, and reproduction in any medium, provided the original author(s) and source are credited.

References

1. Agar J, Durham H (2003) Relevance of oxidative injury in the pathogenesis of motor neuron diseases. Amyotroph Lateral Scler Other Motor Neuron Disord 4:232–242
2. Aizenman E, Lipton SA, Loring RH (1989) Selective modulation of NMDA responses by reduction and oxidation. Neuron 2:1257–1263
3. Aracena-Parks P, Goonasekera SA, Gilman CP, Dirksen RT, Hidalgo C, Hamilton SL (2006) Identification of cysteines involved in S-nitrosylation, S-glutathionylation, and oxidation to disulfides in ryanodine receptor type 1. J Biol Chem 281:40354–40368
4. Avshalumov MV, Patel JC, Rice ME (2008) AMPA receptor-dependent H_2O_2 generation in striatal medium spiny neurons but not dopamine axons: one source of a retrograde signal that can inhibit dopamine release. J Neurophysiol 100:1590–1601
5. Avshalumov MV, Rice ME (2002) NMDA receptor activation mediates hydrogen peroxide-induced pathophysiology in rat hippocampal slices. J Neurophysiol 87:2896–2903
6. Bickler PE, Gallego SM, Hansen BM (1993) Developmental changes in intracellular calcium regulation in rat cerebral cortex during hypoxia. J Cereb Blood Flow Metab 13:811–819
7. Bindokas VP, Jordan J, Lee CC, Miller RJ (1996) Superoxide production in rat hippocampal neurons: selective imaging with hydroethidine. J Neurosci 16:1324–1336
8. Boveris A, Chance B (1973) The mitochondrial generation of hydrogen peroxide. General properties and effect of hyperbaric oxygen. Biochem J 134:707–716
9. Cadenas E, Davies KJ (2000) Mitochondrial free radical generation, oxidative stress, and aging. Free Radic Biol Med 29:222–230
10. Chan PH (2001) Reactive oxygen radicals in signaling and damage in the ischemic brain. J Cereb Blood Flow Metab 21:2–14
11. Choi SE, Min SH, Shin HC, Kim HE, Jung MW, Kang Y (2006) Involvement of calcium-mediated apoptotic signals in H_2O_2-induced MIN6N8a cell death. Eur J Pharmacol 547:1–9
12. Cleland WW (1964) Dithiothreitol, a new protective reagent for SH groups. Biochemistry 3:480–482
13. Davidson SM, Duchen MR (2006) Calcium microdomains and oxidative stress. Cell Calcium 40:561–574
14. Dean RT, Fu S, Stocker R, Davies MJ (1997) Biochemistry and pathology of radical-mediated protein oxidation. Biochem J 324:1–18
15. Desagher S, Glowinski J, Premont J (1996) Astrocytes protect neurons from hydrogen peroxide toxicity. J Neurosci 16:2553–2562
16. Dröge W (2002) Free radicals in the physiological control of cell function. Physiol Rev 82:47–95
17. Duchen MR, Biscoe TJ (1992) Mitochondrial function in type I cells isolated from rabbit arterial chemoreceptors. J Physiol 450:13–31
18. Emaus RK, Grunwald R, Lemasters JJ (1986) Rhodamine 123 as a probe of transmembrane potential in isolated rat-liver mitochondria: spectral and metabolic properties. Biochim Biophys Acta 850:436–448
19. Foster KA, Galeffi F, Gerich FJ, Turner DA, Müller M (2006) Optical and pharmacological tools to investigate the role of mitochondria during oxidative stress and neurodegeneration. Prog Neurobiol 79:136–171
20. Fowler JC (1997) Hydrogen peroxide opposes the hypoxic depression of evoked synaptic transmission in rat hippocampal slices. Brain Res 766:255–258
21. Funke F, Dutschmann M, Müller M (2007) Imaging of respiratory-related population activity with single-cell resolution. Am J Physiol Cell Physiol 292:C508–516
22. Gerich FJ, Hepp S, Probst I, Müller M (2006) Mitochondrial inhibition prior to oxygen-withdrawal facilitates the occurrence of hypoxia-induced spreading depression in rat hippocampal slices. J Neurophysiol 96:492–504
23. Gonzalez A, Granados MP, Pariente JA, Salido GM (2006) H_2O_2 mobilizes Ca^{2+} from agonist- and thapsigargin-sensitive and insensitive intracellular stores and stimulates glutamate secretion in rat hippocampal astrocytes. Neurochem Res 31:741–750
24. Halliwell B (1992) Reactive oxygen species and the central nervous system. J Neurochem 59:1609–1623

25. Hammarström AK, Gage PW (2000) Oxygen-sensing persistent sodium channels in rat hippocampus. J Physiol 529:107–118
26. Hepp S, Gerich FJ, Müller M (2005) Sulfhydryl oxidation reduces hippocampal susceptibility to hypoxia-induced spreading depression by activating BK-channels. J Neurophysiol 94:1091–1103
27. Hepp S, Müller M (2008) Sulfhydryl oxidation: a potential strategy to achieve neuroprotection during severe hypoxia? Neuroscience 152:903–912
28. Hidalgo C, Bull R, Behrens MI, Donoso P (2004) Redox regulation of RyR-mediated Ca^{2+} release in muscle and neurons. Biol Res 37:539–552
29. Hoyt KR, Gallagher AJ, Hastings TG, Reynolds IJ (1997) Characterization of hydrogen peroxide toxicity in cultured rat forebrain neurons. Neurochem Res 22:333–340
30. Huddleston AT, Tang W, Takeshima H, Hamilton SL, Klann E (2008) Superoxide-induced potentiation in the hippocampus requires activation of ryanodine receptor type 3 and ERK. J Neurophysiol 99:1565–1571
31. Joo HJ, Ma JY, Choo YG, Choi BK, Jung KY (1999) Age-related alteration of intracellular ATP maintenance in the cell suspensions of mice cerebral cortex. Mech Ageing Dev 110:1–12
32. Kovács R, Schuchmann S, Gabriel S, Kann O, Kardos J, Heinemann U (2002) Free radical-mediated cell damage after experimental status epilepticus in hippocampal slice culture. J Neurophysiol 88:2909–2918
33. Lamprecht W, Trautschold I (1974) Bestimmung mit hexokinase und glukose-6-phosphat-dehydrogenase. In: Bergmeyer HU (ed) Methoden der enzymatischen Analyse. Verlag Chemie, Weinheim, pp 2151–2160
34. Lipton SA, Choi YB, Takahashi H, Zhang D, Li W, Godzik A, Bankston LA (2002) Cysteine regulation of protein function–as exemplified by NMDA-receptor modulation. Trends Neurosci 25:474–480
35. Lipton SA, Nicotera P (1998) Calcium, free radicals and excitotoxins in neuronal apoptosis. Cell Calcium 23:165–171
36. Malgaroli A, Tsien RW (1992) Glutamate-induced long-term potentiation of the frequency of miniature synaptic currents in cultured hippocampal neurons. Nature 357:134–139
37. Müller M, Mironov SL, Ivannikov MV, Schmidt J, Richter DW (2005) Mitochondrial organization and motility probed by two-photon microscopy in cultured mouse brainstem neurons. Exp Cell Res 303:114–127
38. Müller M, Schmidt J, Mironov SL, Richter DW (2003) Construction and performance of a custom-built two-photon laser scanning system. J Phys D Appl Phys 36:1747–1757
39. Müller W, Bittner K (2002) Differential oxidative modulation of voltage-dependent K^+ currents in rat hippocampal neurons. J Neurophysiol 87:2990–2995
40. Nowicky AV, Duchen MR (1998) Changes in $[Ca^{2+}]_i$ and membrane currents during impaired mitochondrial metabolism in dissociated rat hippocampal neurons. J Physiol 507:131–145
41. Pellmar T (1986) Electrophysiological correlates of peroxide damage in guinea pig hippocampus in vitro. Brain Res 364:377–381
42. Pellmar TC (1987) Peroxide alters neuronal excitability in the CA1 region of guinea-pig hippocampus in vitro. Neuroscience 23:447–456
43. Pellmar TC (1995) Use of brain slices in the study of free-radical actions. J Neurosci Methods 59:93–98
44. Ponsioen B, Zhao J, Riedl J, Zwartkruis F, van der Krogt G, Zaccolo M, Moolenaar WH, Bos JL, Jalink K (2004) Detecting cAMP-induced Epac activation by fluorescence resonance energy transfer: Epac as a novel cAMP indicator. EMBO Rep 5:1176–1180
45. Pysh JJ, Khan T (1972) Variations in mitochondrial structure and content of neurons and neuroglia in rat brain: an electron microscopic study. Brain Res 36:1–18
46. Ralevic V, Burnstock G (1998) Receptors for purines and pyrimidines. Pharmacol Rev 50:413–492
47. Rintoul GL, Filiano AJ, Brocard JB, Kress GJ, Reynolds IJ (2003) Glutamate decreases mitochondrial size and movement in primary forebrain neurons. J Neurosci 23:7881–7888
48. Sah R, Schwartz-Bloom RD (1999) Optical imaging reveals elevated intracellular chloride in hippocampal pyramidal neurons after oxidative stress. J Neurosci 19:9209–9217
49. Salonikidis PS, Zeug A, Kobe F, Ponimaskin E, Richter DW (2008) Quantitative measurement of cAMP concentration using an Epac based FRET-sensor. Biophys J 95:5412–5423
50. Schmidt-Kastner R, Freund TF (1991) Selective vulnerability of the hippocampus in brain ischemia. Neuroscience 40:599–636
51. Schuchmann S, Lückermann M, Kulik A, Heinemann U, Ballanyi K (2000) Ca^{2+}- and metabolism-related changes of mitochondrial potential in voltage-clamped CA1 pyramidal neurons in situ. J Neurophysiol 83:1710–1721
52. Schuchmann S, Müller W, Heinemann U (1998) Altered Ca^{2+} signaling and mitochondrial deficiencies in hippocampal neurons of trisomy 16 mice: a model of Down's syndrome. J Neurosci 18:7216–7231
53. Seutin V, Scuvee-Moreau J, Massotte L, Dresse A (1995) Hydrogen peroxide hyperpolarizes rat CA1 pyramidal neurons by inducing an increase in potassium conductance. Brain Res 683:275–278
54. Skulachev VP (2001) Mitochondrial filaments and clusters as intracellular power-transmitting cables. Trends Biochem Sci 26:23–29
55. Sutko JL, Airey JA, Welch W, Ruest L (1997) The pharmacology of ryanodine and related compounds. Pharmacol Rev 49:53–98
56. Takahashi A, Mikami M, Yang J (2007) Hydrogen peroxide increases GABAergic mIPSC through presynaptic release of calcium from IP3 receptor-sensitive stores in spinal cord substantia gelatinosa neurons. Eur J Neurosci 25:705–716
57. Teepker M, Anthes N, Fischer S, Krieg JC, Vedder H (2007) Effects of oxidative challenge and calcium on ATP-levels in neuronal cells. Neurotoxicology 28:19–26
58. Treiman M, Caspersen C, Christensen SB (1998) A tool coming of age: thapsigargin as an inhibitor of sarco-endoplasmic reticulum Ca^{2+}-ATPases. Trends Pharmacol Sci 19:131–135
59. van der Krogt GN, Ogink J, Ponsioen B, Jalink K (2008) A comparison of donor-acceptor pairs for genetically encoded FRET sensors: application to the Epac cAMP sensor as an example. PLoS ONE 3:e1916
60. Xia R, Stangler T, Abramson JJ (2000) Skeletal muscle ryanodine receptor is a redox sensor with a well defined redox potential that is sensitive to channel modulators. J Biol Chem 275:36556–36561
61. Zheng Y, Shen X (2005) H2O2 directly activates inositol 1, 4, 5-trisphosphate receptors in endothelial cells. Redox Rep 10:29–36
62. Zhu Y, Kimelberg HK (2004) Cellular expression of P2Y and β-AR receptor mRNAs and proteins in freshly isolated astrocytes and tissue sections from the CA1 region of P8–12 rat hippocampus. Brain Res Dev Brain Res 148:77–87
63. Zissimopoulos S, Lai FA (2006) Redox regulation of the ryanodine receptor/calcium release channel. Biochem Soc Trans 34:919–921